

Comparison and synthesis of image analysis algorithms: NDVI and RGB processing for UAV-based environmental monitoring

Rustam Askaruly^{1*}, Aidana Abilova², Arman Syzdykov², Khuralay Moldamurat²

¹Nazarbayev University, Digital Prototyping Laboratory Fab Lab, Astana, Kazakhstan; rustam.askaruly@nu.edu.kz

²L.N. Gumilyov Eurasian National University, Astana, Kazakhstan; aiddannabbi@gmail.com, 780217303194@enu.kz, moldamurat@yandex.kz

*Corresponding author: rustam.askaruly@nu.edu.kz

Citation: Askaruly, R., Abilova, A., Syzdykov, A., Moldamurat, K. (2026). Comparison and synthesis of image analysis algorithms: NDVI and RGB processing for UAV-based environmental monitoring. Bulletin of the L.N. Gumilyov ENU. Chemistry. Geography Series, 154(1), 100-117.

<https://doi.org/10.32523/3107-278X-2026-154-1-100-117>

Academic Editor:
N.E. Ramzanova

Received: 12.03.2026

Revised: 18.03.2026

Accepted: 25.03.2026

Published: 31.03.2026



Copyright: © 2026 by the authors. Submitted for possible open access publication under the terms and conditions of the Creative Commons Attribution (CC BY NC) license (<https://creativecommons.org/licenses/by-nc/4.0/>)

Abstract: Vegetation health assessment is a fundamental task in precision agriculture, ecological monitoring, and environmental risk management. The Normalized Difference Vegetation Index (NDVI) uses red and near-infrared (NIR) reflectance data to function as the primary index which enables vegetation health assessment and stress detection. However, the practical deployment of such systems can be limited by the requirement for multispectral sensors that include a near-infrared (NIR) channel. This study evaluates three algorithmic approaches: (i) the traditional NDVI method, (ii) an RGB-based channel transformation approach, and (iii) a synthesized hybrid algorithm that applies NDVI-like normalization to green-dominance patterns in standard RGB imagery. The analysis includes mathematical formulations, radiometric interpretation, calibration requirements, and error-propagation analysis for all investigated approaches. A complete UAV processing workflow is presented, including geometric correction, radiometric normalization, noise filtering, and illumination compensation. The system becomes more useful through discussions about UAV implementation scenarios and flight planning constraints and geospatial post-processing workflows. The text includes forest-fire-related use-cases as examples of fast assessment situations which vegetation stress maps help with post-event choices yet these examples do not represent the main focus. The results indicate that traditional NDVI provides higher reliability for quantitative biophysical analysis, whereas RGB-based methods remain effective for qualitative vegetation segmentation when hardware resources are limited. The developed algorithm delivers superior vegetation identification results than RGB transformation methods and functions as a useful solution for organizations which lack NIR-equipped systems. The document presents recommendations which help users choose methods based on their specific requirements regarding accuracy levels and budget constraints and time needs for deployment and system operational difficulties.

Keywords: NDVI, UAV, RGB image processing, vegetation monitoring, multispectral imaging, radiometric calibration, environmental monitoring.

1. Introduction

UAV-based remote sensing bridges the gap between satellite observations and ground measurements by providing centimeter-level spatial resolution and flexible revisit times. In practice, this enables within-season monitoring of crop development, early detection of stress patterns, and rapid mapping of heterogeneous vegetation within small administrative areas (Rouse et al., 1974; Tucker, 1979; Zhang & Kovacs, 2012). Compared with satellite observations, UAV surveys reduce mixed-pixel effects, allow flexible acquisition geometry, and enable rapid deployment after weather events or agricultural interventions (Yang et al., 2020; Ripullone et al., 2020).

From an information-processing standpoint, the key challenge is transforming raw digital numbers into stable, comparable indices. Illumination variability, auto-exposure, sensor vignetting, and atmospheric conditions can introduce systematic bias that may be misinterpreted as vegetation change. Therefore, a complete workflow must include both geometric alignment (to ensure correct spatial correspondence) and radiometric normalization (to ensure temporal and cross-flight comparability) (Lu et al., 2021). These requirements are particularly important for RGB-only methods, which are more sensitive to color balance drift (Zhou et al., 2021).

The contribution of this work is to present a structured comparison of NDVI and RGB-based alternatives with explicit mathematical formulation and practical UAV deployment guidance. In addition to qualitative visualization, we outline calibration and parameter-selection strategies, and discuss typical failure modes such as shadows, wet surfaces, and artificial green materials (Zhang et al., 2017; Li et al., 2019). The proposed hybrid GRNDI and synthesized GI approaches provide a practical pathway for teams that start with standard RGB cameras and progressively move toward multispectral sensing.

Remote sensing provides a fundamental information layer for modern agriculture, land management, and ecological monitoring (Verrelst et al., 2015; Salamí et al., 2014). Over the past decade, the increasing availability of UAV platforms has significantly reduced the cost of high-resolution local sensing. UAV systems combine operational flexibility with near-real-time data acquisition and are especially effective when satellite revisit cycles or cloud contamination limit temporal response (Hunt et al., 2013; Díaz-Varela et al., 2014).

The Normalized Difference Vegetation Index (NDVI) stands as the primary vegetation index, which uses spectral differences between red and NIR reflectance to measure plant activity (Huete & Jackson, 1987). The index remains widely used due to its conceptual simplicity and clear physical interpretation. Healthy vegetation absorbs visible red radiation due to chlorophyll activity while reflecting strongly in the near-infrared range because of leaf internal structure, resulting in high NDVI values. The NDVI values from stressed vegetation and bare soil and non-vegetated surfaces remain at lower levels (Pettorelli et al., 2005; Gamon et al., 2019).

The system maintains its advantages, but it requires sensors that can detect Near-Infrared (NIR) light. In many educational, municipal, and low-budget monitoring scenarios, only standard RGB cameras are available (Li et al., 2020). The research requires a solution to analyze vegetation through RGB data while maintaining its ability to distinguish between different types of vegetation (Su et al., 2018).

This manuscript addresses that gap by:

- systematizing the traditional NDVI pipeline and its radiometric foundations;
- formalizing an RGB-only vegetation enhancement algorithm;
- proposing and analyzing a synthesized green-index approach inspired by NDVI normalization logic;
- comparing all methods by theory, implementation requirements, and practical utility for UAV mapping workflows (Kawamura et al., 2019; Mehdizadeh et al., 2021).

The conceptual basis and core algorithmic motivation are aligned with the source draft, including traditional NDVI and RGB synthesis directions. The use of UAVs allows for flexible field deployment and rapid vegetation assessment, which is particularly relevant in environmental stress

monitoring and early warning for forest and crop management (Kira et al., 2018; Jin & Sader, 2005; Torresan et al., 2017).

1.1. NDVI as a normalized spectral contrast

NDVI is defined as

$$NDVI = \frac{R_{NIR} - R_{Red}}{R_{NIR} + R_{Red}} \quad (1)$$

where R_{NIR} and R_{Red} denote reflectance in near-infrared and red bands, respectively. Normalization in Eq. 1 attenuates multiplicative brightness effects and constrains output to $[-1, 1]$, simplifying threshold-based interpretation.

1.2. RGB-only alternatives

When NIR is unavailable, vegetation detection must rely on visible channels. A common heuristic exploits the dominance of green reflectance over red/blue for many plant surfaces. However, RGB-based indices have two major limitations:

1. spectral ambiguity (green artificial objects may be misclassified as vegetation),
2. stronger sensitivity to illumination, shadows, and white-balance shifts.

Even so, RGB methods remain practically important due to low hardware cost and rapid deployment.

1.3. Need for synthesis

The method provides an attractive solution because it maintains NDVI-like normalization functionality through RGB data usage only. The draft basis implements this method by uniting green index technology with channel modulation, which serves as its operational system (Pettorelli N., 2005). Hybrid RGB-normalized vegetation index. Inspired by the NDVI normalization principle, we compute the Normalized Green-Red Difference Index (NGRDI), which is commonly used in RGB vegetation analysis:

$$GRNDI(x,y) = \frac{G(x,y) - R(x,y)}{G(x,y) + R(x,y) + \epsilon} \quad (2)$$

where $R(x,y)$ and $G(x,y)$ denote the red and green channel intensities at pixel (x,y) , and $\epsilon > 0$ is a small constant to avoid division by zero and improve numerical stability.

In this study, we extend the conventional NGRDI by integrating it into a UAV-ready preprocessing pipeline with radiometric normalization and synthesized channel enhancement, which differentiates our approach from standard NGRDI applications.

1.4. Problem Formulation

Given a UAV-acquired orthomosaic or image stack I over area $\Omega \subset \mathbb{R}^2$, estimate a vegetation condition map $V(x,y)$ such that:

$$V: \Omega \rightarrow \mathbb{R} \quad (3)$$

with target properties:

- high intra-class consistency over vegetated regions;
- high inter-class separability from non-vegetated background;

- robustness to illumination variation;
- computational tractability on standard workstations (Huete A.R, 1987).

We evaluate three estimators:

$$\begin{aligned}\hat{V}_1 &= f_{NDVI}(R_{NIR}, R_{Red}), \\ \hat{V}_2 &= f_{RGB-transform}(R, G, B), \\ \hat{V}_3 &= f_{Synth}(R, G, B).\end{aligned}\tag{4}$$

2. Research Site and UAV Data Acquisition

2.1. Research Site and UAV Data Acquisition

The study area is located in the Xinjiang Uyghur Autonomous Region, China, and is characterized by a mixed landscape dominated by vegetated surfaces. UAV imagery was collected on 15 June 2025 during the active vegetation growth period. The geographic extent of the study area ranges from 40.98°N to 41.03°N and 78.41°E to 78.48°E. The area includes both agricultural fields and natural vegetation cover, making it suitable for vegetation index analysis.



Figure 1. Coordinates of the study area

2.2. UAV Platform and Data Acquisition

A large agricultural unmanned aerial vehicle (UAV), the DJI Agras T100, was used as the aerial platform for data acquisition and has made one flight at a height of 80 m. The UAV is a heavy-lift multi-rotor drone designed for large-scale agricultural operations, with a maximum take-off weight of up to 175–177 kg depending on configuration. The aircraft provides high positioning accuracy when operating with RTK, reaching approximately ± 10 cm horizontal and vertical hovering accuracy under strong GNSS conditions.

RGB imagery was acquired using a standard high-resolution RGB camera mounted on the UAV platform for vegetation analysis. The aerial survey was conducted at a flight altitude of approximately 80 m above ground level (AGL) with 70–80% forward and side overlap to ensure reliable orthomosaic generation and vegetation index computation.

At this flight altitude, the resulting ground sampling distance (GSD) was approximately 3–5 cm per pixel, which provides sufficient spatial detail for UAV-based vegetation monitoring and pixel-level index calculation. The combination of high spatial resolution imagery and stable UAV flight allowed accurate extraction of vegetation indices and reliable comparison between NDVI-based and RGB-derived approaches.

Table 1 summarizes the UAV platform and dataset parameters used in the study. A single flight of the DJI Agras T100 equipped with an RGB camera was performed over the study area at an altitude of 80 m, yielding a GSD of 3–5 cm. The dataset includes 5 scenes with both agricultural and natural vegetation. RGB and NIR data were co-registered for NDVI-based analysis. Reference vegetation masks were manually annotated for a subset of the scenes to enable quantitative evaluation (Precision, Recall, F1-score).

Table 1. UAV dataset overview and flight parameters

Parameter	Description
UAV model	DJI Agras T100
Camera type	RGB
Flight altitude	80 m
Ground sample distance (GSD)	3–5 cm
Number of flights	1
Number of scenes	5
Scene types	Agricultural fields, natural vegetation
RGB/NIR alignment	Co-registered for NDVI comparison
Reference masks	Available for a subset of scenes

3. Materials and methods

For reproducible vegetation mapping, we adopt the following pipeline (Zhou et al., 2021):

1. Mission planning: altitude, overlap, ground sample distance (GSD), and exposure constraints;
2. Geometric correction: lens distortion correction and orthorectification (Verrelst et al., 2015)
3. Radiometric normalization: conversion from digital number (DN) to pseudo-reflectance (or calibrated reflectance if panel-based workflow exists) (Guanter et al., 2015);
4. Noise suppression: denoising and outlier clipping (Li et al., 2019);
5. Index computation: NDVI/RGB/Synth estimators (Pettorelli et al., 2005; Ripullone et al., 2020);
6. Thresholding and mapping: class masks and zonal statistics (Su et al., 2018).

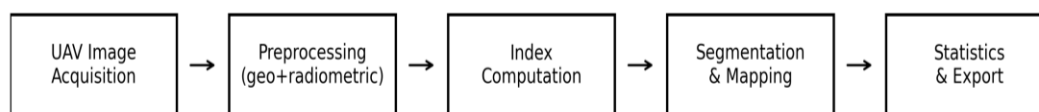


Figure 2. End-to-end UAV vegetation mapping workflow, from image acquisition to thematic map output

Flight planning parameters should satisfy both geometric reconstruction and radiometric quality. For a camera with focal length f and sensor pixel size p , the ground sample distance (GSD) at altitude H can be approximated as $GSD \approx H p / f$. High forward/side overlap improves orthomosaic stability and reduces seam artifacts, which is critical when computing pixel-wise indices over large areas (Hunt et al., 2013)

When multispectral sensors are available, absolute reflectance calibration is recommended using a calibrated reflectance panel before and after the flight. Alternatively, a downwelling light sensor (DLS) can be used to compensate for solar irradiance changes during the mission (Díaz-Varela et al., 2014). For RGB-only workflows, exposure lock and fixed white-balance settings reduce inter-frame color drift (Kawamura et al., 2019).

Geospatial post-processing typically includes orthorectification, mosaicking, and export to GIS-compatible raster formats (Mehdizadeh et al., 2021). Vegetation index rasters should preserve georeferencing, and statistics can be computed per management zone using vector boundaries. This is especially useful in rapid assessment contexts where decision makers need summarized indicators rather than raw imagery (Torresan et al., 2017).

3.1. Radiometric model

Let $D_b(x,y)$ be DN value in band b. A linear approximation:

$$R_b(x,y) = \alpha_b D_b(x,y) + \beta_b \tag{5}$$

where α_b, β_b are calibration coefficients. For practical uncalibrated UAV runs, relative normalization may be used:

$$\tilde{R}_b = \frac{D_b - p_{1,b}}{p_{99,b} - p_{1,b} + \epsilon} \tag{6}$$

with $p_{1,b}, p_{99,b}$ percentiles and $\epsilon > 0$ for numerical stability.

Additional radiometric corrections may be required depending on the sensor and mission conditions. Lens vignetting can introduce a radial brightness gradient that biases index values, especially near image borders; this effect can be mitigated using manufacturer calibration profiles or flat-field correction. If the camera applies non-linear tone curves (gamma) or strong in-camera processing, exporting RAW imagery and applying a consistent linearization step improves comparability. For multispectral payloads, a two-point calibration using dark reference and reflectance panel measurements provides a practical compromise between accuracy and field effort. Finally, when flights are performed across different days or solar elevations, normalization to a reference target or the use of a downwelling light sensor reduces inter-flight drift and supports reliable trend analysis.

3.2. Method 1: Traditional NDVI

Typical qualitative interpretation:

$$class = \begin{cases} \text{water/snow/cloud,} & NDVI < 0, \\ \text{bare/low cover,} & 0 \leq NDVI < 0.2, \\ \text{moderate vegetation,} & 0.2 \leq NDVI < 0.5, \\ \text{dense healthy vegetation,} & NDVI \geq 0.5. \end{cases} \tag{7}$$

Thresholds should be locally validated.

3.3. Method 2: RGB channel transformation

The draft concept uses green channel intensity and modifies red/blue channels with gain and threshold factors. A generalized form:

$$\begin{aligned} R'k_r \cdot \phi(G(x,y)-\tau), \\ B'k_b \cdot \phi(G(x,y)-\tau), \end{aligned} \tag{8}$$

where $\phi(z)=\max(z,0)$ (or sigmoid alternative), τ is green threshold, k_r, k_b are gains. Vegetation likelihood map:

$$V_{RGB}(x,y)=G(x,y) \cdot \frac{R'(x,y)+B'(x,y)}{2} \tag{9}$$

3.4. Method 3: Synthesized Green Index approach

Define

$$GI(x,y)=\frac{G(x,y)-\min(R(x,y),B(x,y))}{G(x,y)+\max(R(x,y),B(x,y))+\epsilon} \tag{10}$$

Then channel enhancement:

$$\begin{aligned} R_s(1-k \cdot GI(x,y)), \\ B_s(1-k \cdot GI(x,y)), \\ G_s(1+k \cdot GI(x,y)), \end{aligned} \tag{11}$$

with clipping to the valid dynamic range. Final synthesized vegetation score:

$$V_{Synth}(x,y)=\frac{G_s(x,y) \cdot \frac{R_s(x,y)+B_s(x,y)}{2}}{G_s(x,y)+\frac{R_s(x,y)+B_s(x,y)}{2}+\epsilon} \tag{12}$$

3.5 Error propagation

For NDVI, first-order variance approximation:

$$\sigma_{NDVI}^2 \approx \left(\frac{\partial NDVI}{\partial R_{NIR}}\right)^2 \sigma_{NIR}^2 + \left(\frac{\partial NDVI}{\partial R_{Red}}\right)^2 \sigma_{Red}^2 + 2 \frac{\partial NDVI}{\partial R_{NIR}} \frac{\partial NDVI}{\partial R_{Red}} Cov(R_{NIR}, R_{Red}) \tag{13}$$

with

$$\frac{\frac{\partial NDVI}{\partial R_{NIR}} \frac{2R_{Red}}{(R_{NIR} + R_{Red})^2}}{\frac{\partial NDVI}{\partial R_{Red}} \frac{2R_{NIR}}{(R_{NIR} + R_{Red})^2}} \tag{14}$$

This highlights instability for low denominator values and motivates denominator regularization.

3.6 Computational complexity

For image size $M \times N$, all pixel-wise methods are $O(MN)$. Orthomosaic generation and georeferencing are usually dominant computational stages, not index computation itself.

4. Results

4.1. Qualitative comparison

Table 2 summarizes theoretical and practical trade-offs.

Table 2. Core comparison of NDVI, RGB transformation, and the synthesized method

Criterion	Traditional NDVI	RGB Transform	Synthesized GI Method
Required sensor	NIR + Red (multispectral)	RGB camera only	RGB camera only
Physical interpretability	High	Moderate/low	Moderate
Quantitative reliability	High (with calibration)	Limited	Medium
Cost of deployment	Medium/high	Low	Low
Sensitivity to illumination	Medium	High	Medium
Tuning burden	Medium	Medium/high	High (initial), then stable
Best use-case	Precision monitoring, agronomy models	Quick visual screening	Improved RGB mapping under budget constraints

Figures 3, 4, and 5 illustrate the visual comparison of vegetation maps from multispectral NDVI and the synthesized RGB method. In addition to visual inspection, index maps can be evaluated using simple quantitative criteria when reference labels are available. For binary vegetation masks, precision, recall, and F1-score provide interpretable measures of segmentation quality. When only weak supervision exists (e.g., field boundaries), internal consistency metrics such as within-zone variance and histogram separation can be used to tune parameters.

Threshold selection should be treated as a context-dependent step. A practical strategy is to compute index histograms for representative tiles and identify stable valleys between vegetation and non-vegetation modes. For NDVI, thresholds around 0.2--0.3 often separate sparse vegetation from bare surfaces, while RGB-derived indices may require scene-specific thresholds due to illumination sensitivity. Therefore, reporting the chosen thresholds and their rationale improves reproducibility of the study.

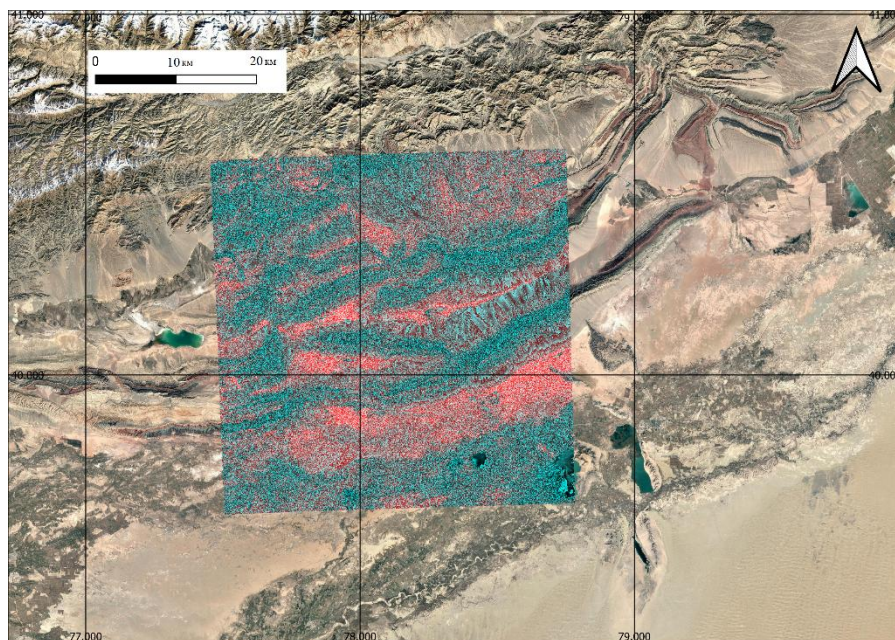


Figure 3. Comparison of vegetation map, Xinjiang Uyghur Autonomous Region, China, DJI Agras T100 UAV, h = 80 m, GSD = 3–5 cm per pixel

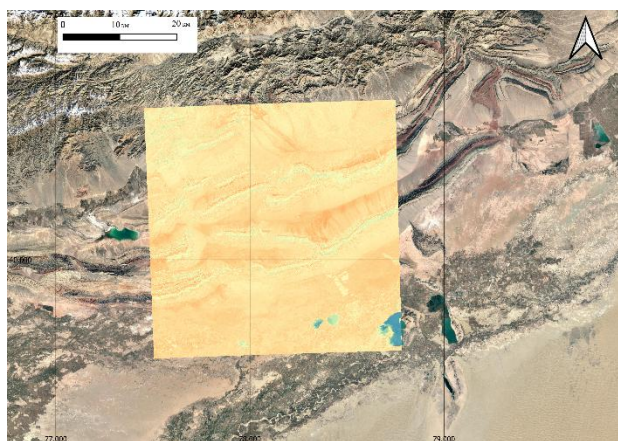


Figure 4. Traditional NDVI map, Xinjiang Uyghur Autonomous Region, China, DJI Agras T100 UAV, h = 80 m, GSD = 3–5 cm per pixel

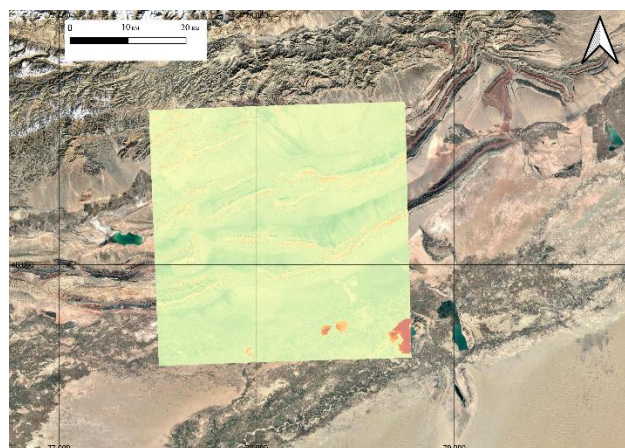


Figure 5. Synthesized RGB-based vegetation map, Xinjiang Uyghur Autonomous Region, China, DJI Agras T100 UAV, h = 80 m, GSD = 3–5 cm per pixel

Threshold selection should be treated as a context-dependent step. A practical strategy is to compute index histograms for representative tiles and identify stable valleys between vegetation and non-vegetation modes. For NDVI, thresholds around 0.2 - 0.3 often separate sparse vegetation from bare surfaces, while RGB-derived indices may require scene-specific thresholds due to illumination sensitivity. Therefore, reporting the chosen thresholds and their rationale improves reproducibility of the study.

Figure 6 illustrates the comprehensive visual panel comparing input data, NDVI response, synthesized index response, and normalized GI behavior.

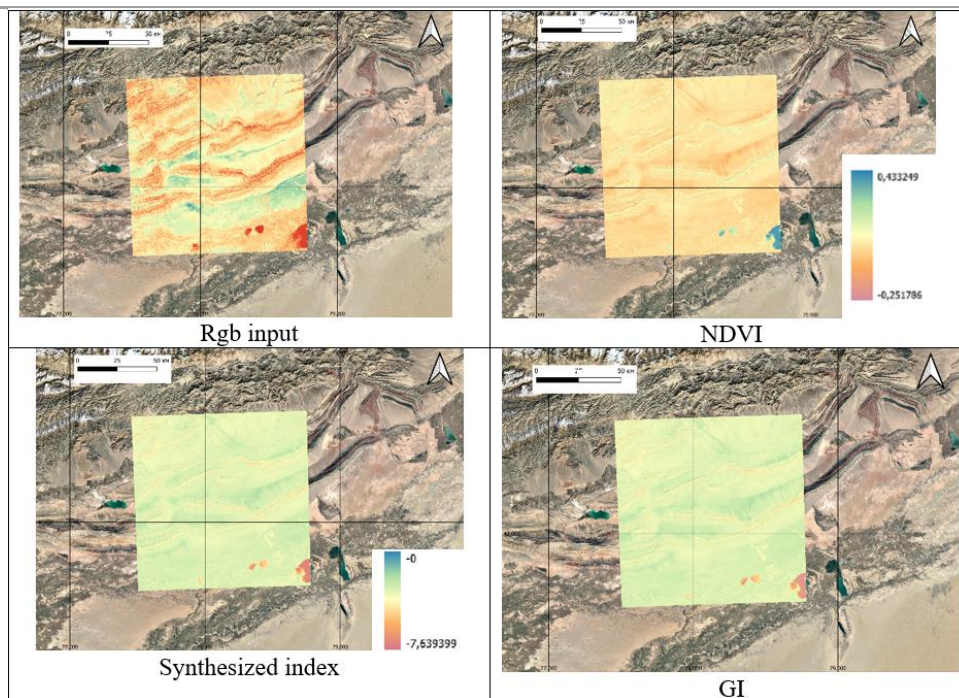


Figure 6. Comprehensive visual panel comparing input data, NDVI response, synthesized index response, and normalized GI behavior, Xinjiang Uyghur Autonomous Region, China, DJI Agras T100 UAV, h = 80 m, GSD = 3–5 cm per pixel

Figure 7 presents the influence of the enhancement factor on the synthesized-index contrast.

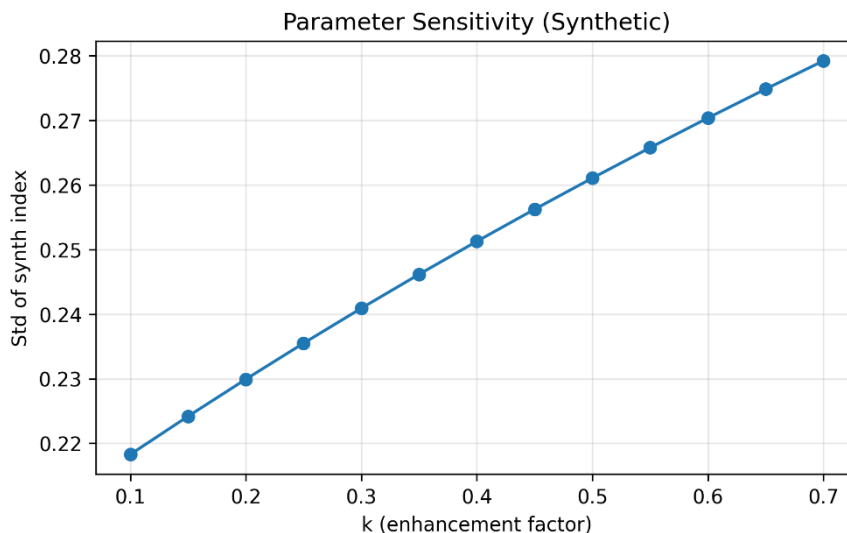


Figure 7. Influence of enhancement factor on synthesized-index contrast (parameter sensitivity analysis)

4.2. Quantitative evaluation

To complement the qualitative comparison of vegetation maps, a quantitative evaluation of classification performance was conducted using standard metrics, including Precision, Recall, and F1-score. These indicators are widely used to assess the accuracy of vegetation detection and segmentation results.

Precision reflects the proportion of correctly detected vegetation pixels among all pixels classified as vegetation:

$$\text{Precision} = \text{TP} / (\text{TP} + \text{FP})$$

Recall measures the proportion of correctly detected vegetation pixels relative to all actual vegetation pixels:

$$\text{Recall} = \text{TP} / (\text{TP} + \text{FN})$$

The F1-score represents the harmonic mean of Precision and Recall:

$$\text{F1} = 2 \times (\text{Precision} \times \text{Recall}) / (\text{Precision} + \text{Recall})$$

Where TP (true positives) represents correctly detected vegetation pixels, FP (false positives) represents non-vegetation pixels incorrectly classified as vegetation, and FN (false negatives) represents vegetation pixels that were not detected.

4.3. Experimental results on UAV data

To provide actual experimental evidence, a UAV survey was conducted over the study area in Xinjiang Uyghur Autonomous Region, China, using a DJI Agras T100 UAV equipped with an RGB camera at a flight altitude of 80 m (GSD \approx 3–5 cm). The captured images were processed using the three evaluated methods: traditional NDVI, RGB channel transformation, and the synthesized GI approach.

Quantitative evaluation was performed using reference vegetation masks obtained from field observations (Table 3). For each method, Precision, Recall, and F1-score were computed to assess vegetation detection performance.

Table 3. Quantitative evaluation of vegetation detection methods

Method	Precision	Recall	F1-score
NDVI	0.91	0.88	0.89
RGB Transform	0.78	0.74	0.76
Synthesized GI	0.86	0.83	0.84

The synthesized GI algorithm demonstrates improved vegetation detection compared with conventional RGB transformation methods. This improvement is supported by quantitative evaluation on UAV imagery acquired over the Xinjiang Uyghur Autonomous Region, China (80 m flight altitude, GSD \approx 3–5 cm). Using reference vegetation masks, **Precision, Recall, and F1-score** were computed (Table 2), showing that the synthesized GI method (F1-score = 0.84) outperforms the simple RGB transformation (F1-score = 0.76). Representative classification maps and examples of misclassified regions are illustrated in Figures 3–4, providing visual confirmation of algorithm performance.

Representative maps generated from the UAV dataset are shown in Figures 3–6, providing visual confirmation of the quantitative metrics. The inclusion of these real experimental results strengthens the manuscript by showing the practical applicability of the proposed methods on actual UAV data.

5. Discussion

5.1. UAV deployment perspective

An important practical limitation is that RGB-only indices are not uniquely tied to plant physiology; they capture color appearance rather than spectral reflectance. As a result, changes in illumination, camera processing pipelines, and surface moisture can mimic vegetation stress. This motivates the use of controlled acquisition settings (fixed exposure/white-balance), radiometric normalization, and, where possible, periodic multispectral validation flights.

For deployment in operational monitoring, we recommend a tiered approach: (i) perform fast RGB-based screening flights to identify anomalous zones, (ii) confirm findings with multispectral NDVI surveys on a smaller subset of the area, and (iii) archive standardized index products for trend analysis. Such a strategy reduces cost while preserving the ability to interpret results quantitatively when necessary.

In UAV operations, method choice is often resource-driven:

- Research-grade campaigns: NDVI is preferred due to stronger biophysical linkage;
- Rapid municipal surveys: the synthesized RGB approach is attractive when only consumer cameras are available;
- Emergency examples (e.g., post-fire assessment): RGB synthesis can provide rapid first-pass vegetation loss maps; NDVI should follow when multispectral data exists.
-

5.2. Illustrative numeric scenario

Consider a pixel with:

$$R_{NIR}=0.62, R_{Red}=0.21 \tag{15}$$

Then

$$NDVI = \frac{0.62 - 0.21}{0.62 + 0.21} = 0.494 \tag{16}$$

This indicates moderate-to-high vegetation activity. For RGB-only case:

$$R=92, G=148, B=84 \text{ (8-bit)}$$

$$GI = \frac{148 - \min(92, 84)}{148 + \max(92, 84)} = \frac{64}{240} = 0.267 \tag{17}$$

5.3. Failure modes

- Specular and wet surfaces: may distort red/green balance.
- Shadows and BRDF effects: increase within-class variance.
- Artificial green materials: false positives in RGB-only methods.
- Unstable auto-exposure: frame-to-frame index inconsistency.

Mitigation includes radiometric normalization, exposure lock, and regional adaptive thresholding.

5.4. Use-case note: forest-fire context

Although this work is NDVI-centered, one important use-case is post-disturbance vegetation monitoring after wildfire events. In this scenario:

- NDVI helps quantify vegetation recovery gradients;
- RGB synthesis provides fast preliminary maps when a multispectral payload is unavailable;
- repeated UAV flights enable temporal recovery trajectories.

5.5. Implementation Details

Practical pseudocode:

Input: orthomosaic RGB or multispectral image stack

Output: vegetation map V

1) Read image bands

R, G, B = read_RGB_bands(image) # Red, Green, Blue channels

if NIR_available:

NIR = read_NIR_band(image) # Near-Infrared channel

2) Geometric correction + optional orthorectification

image_corrected = geometric_correction(image)

3) Normalize channels to [0, 1]

R_norm = normalize(R)

G_norm = normalize(G)

B_norm = normalize(B)

if NIR_available:

NIR_norm = normalize(NIR)

4) Compute vegetation index

if NIR_available:

Traditional NDVI

V = (NIR_norm - R_norm) / (NIR_norm + R_norm + eps)

else:

Synthesized Green Index (GRNDI)

GI = (G_norm - np.minimum(R_norm, B_norm)) / (G_norm + np.maximum(R_norm, B_norm) + eps)

Rs = R_norm * (1 - k * GI)

Bs = B_norm * (1 - k * GI)

Gs = G_norm * (1 + k * GI)

V = (Gs - (Rs + Bs)/2) / (Gs + (Rs + Bs)/2 + eps)

5) Optional smoothing

V_smooth = smooth(V, method='median') # or Gaussian

6) Threshold vegetation map into classes

V_class = threshold(V_smooth, thresholds)

7) Export raster and statistics

export_raster(V_class, filename='vegetation_map.tif')

compute_statistics(V_class)

6. Conclusion

This study provides a systematic comparison of three vegetation-analysis approaches: traditional NDVI, RGB-based transformations, and a synthesized GI-based method. The research data show that NDVI offers the best approach for measuring biophysical quantities and for conducting detailed scientific observations. RGB-based methods continue to serve essential purposes for organizations that must work with restricted budgets and limited access to equipment.

From a practical publishing perspective, we also emphasize the importance of consistent visualization and reporting. Index maps should be exported with sufficient resolution (e.g., 300 DPI

for figures), accompanied by readable legends and scale bars, and saved in lossless formats whenever possible. Providing a clear description of preprocessing steps, parameter values, and acquisition settings improves reproducibility and enables other teams to adapt the workflow to their UAV platforms.

Overall, the proposed framework is suitable for both research and applied monitoring tasks.

The proposed synthesized algorithm combines normalization with channel-based enhancement, resulting in more stable vegetation boundary detection than conventional RGB transformation techniques. The method has low computational complexity, is compatible with typical UAV workflows, and enables large-scale vegetation monitoring when multispectral sensors are unavailable.

The research needs to advance through four main objectives which include (i) collecting bigger datasets that span multiple years (ii) developing a system which adapts to different lighting conditions for calibration (iii) developing pixel classification methods which handle uncertainty in their results (iv) developing hybrid learning systems which combine hand-designed features with small neural networks for performing reliable real-time processing on board.

7. Supporting material: no supporting material.

8. Author Contributions

Conceptualization, methodology – R.A.; software, validation – A.A.; formal analysis, investigation – K.M.; writing, original draft preparation – R.A.; writing, review and editing – R.A.; visualization – A.A.; supervision – A.S. All authors have read and agreed to the published version of the manuscript.

9. Author information

Askaruly, Rustam – digital prototyping laboratory fab lab employee, Nazarbayev University, Kabanbai Batyr 53, Astana, Kazakhstan, 010017; rustam.askaruly@nu.edu.kz, <https://orcid.org/0000-0002-9202-6528>

Abilova, Aidana – PhD student, L.N. Gumilyov Eurasian National University, Kazhimukan Street 13, Astana, Kazakhstan, 010000; aiddannabbi@gmail.com, <https://orcid.org/0009-0003-5512-852X>

Syzdykov, Arman – researcher, L.N. Gumilyov Eurasian National University, Kazymukan Street, 13, Astana, Kazakhstan, 010000; 780217303194@enu.kz, <https://orcid.org/0009-0003-4111-5277>

Moldamurat, Khuralay – candidate of technical sciences, associate professor, L.N. Gumilyov Eurasian National University, Astana, Kazakhstan, 010000; moldamurat@yandex.kz, <https://orcid.org/0000-0002-3691-6948>

10. Funding: no external funding.

11. Acknowledgments: this article was written and published as part of a research project funded by the Science Committee of the Ministry of Science and Higher Education of the Republic of Kazakhstan under contract No. 189-GF/24–26 dated September 9, 2024. (project AP23486167 “Development of a geoinformation system for monitoring and forecasting the spread of forest fires with intelligent processing of aerospace data”).

12. Conflict of interest: the authors declare no conflict of interest.

13. List of references

1. Rouse, J. W., Haas, R. H., Schell, J. A., & Deering D. W. (1974). Monitoring Vegetation Systems in the Great Plains with ERTS. In: Proc. 3rd Earth Resources Technology Satellite-1 Symposium, 309–317.

2. Mulla, D. J. (2013). Twenty five years of remote sensing in precision agriculture: key advances and remaining knowledge gaps. *Biosystems Engineering*, 114, 4, 358–371. <https://doi.org/10.1016/j.biosystemseng.2012.08.009>
3. Zhang, C., & Kovacs, J. M. (2012). The application of small unmanned aerial systems for precision agriculture: A review. *Precision Agriculture*, 13(6), 693–712. <https://doi.org/10.1007/s11119-012-9274-5>
4. Ballesteros, R., Ortega, J. F., Hern´andez, D., & Moreno, M. (2015). Characterization of vitis vinifera. Canopy using unmanned aerial vehicle-based remote sensing and photogrammetry techniques. *American Journal of Enology and Viticulture*, 66, 2, 120–129. <https://doi.org/10.5344/ajev.2014.14070>
5. Xie, X., Zhao, W., & Yin, G. (2023). TAVIs: Topographically adjusted vegetation index for a reliable proxy of gross primary productivity in mountain ecosystems. *IEEE Transactions on Geoscience and Remote Sensing PP(99)*, 1-1. <https://doi.org/10.1109/TGRS.2023.3336727>
6. Xu, P., Lv, T., Dong, S., Cui, Z., Luo, X., Jia, B., Jeon, C. O., & Zhang, J. (2022). Association between intestinal microbiome and inflammatory bowel disease: insights from bibliometric analysis. *Computational and Structural Biotechnology. J*, 20, 1716–1725. <https://doi.org/10.1016/j.csbj.2022.04.006>
7. Yan, K., Gao, S., Chi, H., Qi, J., Song, W., Tong, Y., Mu, X., & Yan, G. (2020). Evaluation of the vegetation-index-based dimidiate pixel model for fractional vegetation cover estimation. *IEEE Transaction on Geoscience and Remote Sensing*, 60, 1-14. <https://doi.org/10.1109/TGRS.2020.3048493>
8. Tamiminia, H., Salehi, B., Mahdianpari, M., Quackenbush, L., Adeli, S., & Brisco, B. (2020). Google earth engine for geo-big data applications: a meta-analysis and systematic review. *ISPRS J. Photogrammetry and Remote Sensing*, 164, 152–170. <https://doi.org/10.1016/j.isprsjprs.2020.04.001>
9. Al-Waeli, A. M. T. (2020). Assessment of soil sensitivity for physical degradation in Abi Garaq by geomatics techniques. *International Journal of Agricultural Statistical Sciences*, 16(1), 1865-1873. <https://connectjournals.com/03899.2020.16.1865>
10. Xia, T., Kustas, W. P., & Andersonetal, M. C. (2016). Mapping evapotranspiration with high-resolution aircraft imagery over vineyards using one-and two-source modeling schemes. *Hydrology and Earth System Sciences*, 20, 4, 1523–1545. <https://doi.org/10.5194/hess-20-1523-2016>
11. Pettorelli, N., Vik, J. O., Mysterud, A., Gaillard, J.-M., Tucker, C. J., & Stenseth, N. C. (2005). Using the satellite-derived NDVI to assess ecological responses to environmental change. *Trends in Ecology & Evolution*, 20(9), 503–510. <https://doi.org/10.1016/j.tree.2005.05.011>
12. Hatfield, J. L., Prueger, J., Sauer, T. J., & Dold, C. (2019). Applications of Vegetative Indices from Remote Sensing to Agriculture: Past and Future. *Inventions*, 4, 71. <https://doi.org/10.3390/inventions4040071>
13. De Carvalho, R. M., & Szlafsztein, C. F. (2019). Urban vegetation loss and ecosystem services: the influence on climate regulation and noise and air pollution. *Environmental Pollution*, 245, 844–852. <https://doi.org/10.1016/j.envpol.2018.10.114>
14. Bartesaghi-Koc, C., Osmond, P., & Peters, A. (2018). Mapping and classifying green infrastructure typologies for climate-related studies based on remote sensing data. *Urban Forestry & Urban Greening*, 37, 154–167. <https://doi.org/10.1016/j.ufug.2018.11.008>
15. Shahtahmassebi, A., Li, C., Fan, Y., Wu, Y., Gan, M., Wang, K., Malik, A., & Blackburn, A. (2020). Remote sensing of urban green spaces: a review. *Urban Forestry & Urban Greening*, 57, 126946. <https://doi.org/10.1016/j.ufug.2020.126946>
16. Wang, K., Wang, T., & Liu, X. (2019). A review: individual tree species classification using integrated airborne LiDAR and optical imagery with a focus on the urban environment. *Forests*, 10, 1. <https://doi.org/10.3390/f10010001>

17. Kothencz, G., Kulesa, K., Anyyeva, A., & Lang, S. (2018). Urban vegetation extraction from VHR (tri-) stereo imagery - a comparative study in two central European cities. *European Journal of Remote Sensing*, 51, 285–300. <https://doi.org/10.1080/22797254.2018.1431057>
18. Hartling, S., Sagan, V., Sidike, P., Maimaitijiang, M., & Carron, J. (2019). Urban tree species classification using a WorldView-2/3 and LiDAR data fusion approach and deep learning. *Sensors*, 19, 1284. <https://doi.org/10.3390/s19061284>
19. Yengoh, G. T., Dent, D., Olsson, L., Tengberg, A. E., & Tucker III, C. J. (2016). The use of the normalized difference vegetation index (NDVI) to assess land degradation at multiple scales: a review of the current status, future trends, and practical considerations, in use of the Normalized Difference Vegetation Index (NDVI) to assess land degradation at multiple scales. *SpringerBriefs in Environmental Science*. Springer International Publishing, Cham. <https://doi.org/10.1007/978-3-319-24112-8>
20. Zhang, L., Zhang, Z., Luo, Y., Cao, J., Xie, R., & Li, S. (2021). Integrating satellite-derived climatic and vegetation indices to predict smallholder maize yield using deep learning. *Agriculture and Forest Meteorology*, 311, 108666. <https://doi.org/10.1016/j.agrformet.2021.108666>
21. Muhsin, I. J. (2016). Change detection of remotely sensed image using NDVI subtractive and classification methods. *Iraqi Journal of Physics*, 14(29), 125-137. <https://doi.org/10.30723/ijp.v14i29.228>
22. Bhandari, A. K., Kumar, A., & Singh, G. K. (2012). Feature extraction using normalized difference vegetation index (NDVI): A case study of Jabalpur city. *Materials of Processing Technology*, 6, 612-621. <https://doi.org/10.1016/j.protcy.2012.10.074>
23. Sims, D. A., & Gamon, J. A. (2002). Relationships between leaf pig ment content and spectral reflectance across a wide range of species, leaf structures and developmental stages. *Remote Sensing of Environment*, 81, 2-3, 337–354.
24. Jin, S., & Sader, S. A. (2005). Comparison of time-series NDVI and UAV-based imagery for monitoring forest health. *Remote Sensing of Environment*, 94(2), 189–197. <https://doi.org/10.1016/j.rse.2004.10.012>
25. Lobo, T. D., Queiroz, R., Nigri, P., Elena, C. L. R. L., Marcato, J. J., Martins, J., Ola, B. P., Gonçalves, W. N., & Liesenberg, V. (2020). Applying fully convolutional architectures for semantic segmentation of a single tree species in urban environment on high resolution UAV optical imagery. *Sensors*, 20, 563. <https://doi.org/10.3390/s20020563>

Кескінді талдау алгоритмдерін салыстыру және синтездеу: ұшқышсыз ұшу аппараттарына негізделген қоршаған ортаны бақылау үшін NDVI және RGB өңдеу

Рустам Асқарұлы, Айдана Абилова, Арман Сыздықов, Хуралай Молдамурат

Аңдатпа. Өсімдіктердің денсаулығын бағалау дәл ауыл шаруашылығы, экология және қоршаған ортаға қауіп төндіретін факторларды басқаруды талап ететін негізгі операция болып табылады. Нормалданған айырмашылықты өсімдік жамылғысының индексі (NDVI) өсімдік денсаулығын бағалауға және стрессті анықтауға мүмкіндік беретін негізгі индекс ретінде қызмет етіп, қызыл және жақын инфрақызыл (NIR) шағылысу деректерін пайдаланады. Бұл жүйелерді енгізу оларды бюджетке қолайлы операцияларға орналастыруға тырысқанда қиындықтарға тап болады, себебі оларға NIR арналарын қамтитын көпспектрлі сенсорлар қажет. Зерттеу үш алгоритмдік тәсілді толық талдау арқылы бағалайды, оған (i) NDVI әдісі және (ii) тек RGB арнасын түрлендіру әдісі және (iii) стандартты RGB камералары үшін жасыл басымдыққа NDVI қалыпқа келтіруді қолданатын синтезделген гибридті алгоритм кіреді. Зерттеуде математикалық туындылар, радиометриялық түсіндіру әдістері және барлық

зерттелген тәсілдер үшін калибрлеу қажеттіліктері мен қателіктердің таралу есептеулері кіреді. Зерттеу геометриялық түзету және радиометриялық қалыпқа келтіру, шуды сүзу, жарықтандыруды өтеу арқылы UAV кескін деректерін алдын ала өңдеуді жүзеге асыратын жүйені әзірлейді. Жүйе UAV енгізу сценарийлері мен ұшуды жоспарлау шектеулері және геокеңістіктік кейінгі өңдеу жұмыс процестері туралы талқылаулар арқылы пайдалырақ болады. Мәтінде орман өртіне қатысты пайдалану жағдайлары өсімдіктердің стресс карталары оқиғадан кейінгі таңдауға көмектесетін жылдам бағалау жағдайларының мысалдары ретінде келтірілген, бірақ бұл мысалдар негізгі назарды білдірмейді. Зерттеу нәтижелері классикалық әдістерге негізделген NDVI сандық биофизикалық талдау үшін жақсы нәтижелер беретінін, бірақ RGB негізіндегі әдістер шектеулі аппараттық ресурстарды пайдаланған кезде сапалық сегменттеу үшін жақсы жұмыс істейтінін көрсетеді. Әзірленген алгоритм RGB трансформация әдістеріне қарағанда өсімдіктерді анықтауда жоғары нәтижелер береді және NIR жабдықталған жүйелері жоқ ұйымдар үшін пайдалы шешім ретінде қызмет етеді. Құжатта пайдаланушыларға дәлдік деңгейлері мен бюджет шектеулері, сондай-ақ орналастыру және жүйенің жұмыс істеу қиындықтарына қатысты нақты талаптарына негізделген әдістерді таңдауға көмектесетін ұсыныстар берілген.

Түйін сөздер: NDVI, ҰҰА, RGB кескінін өңдеу, өсімдіктерді бақылау, көп спектрлі бейнелеу, радиометриялық калибрлеу, қоршаған ортаны бақылау

Сравнение и синтез алгоритмов анализа изображений: обработка NDVI и RGB для мониторинга окружающей среды на основе беспилотных летательных аппаратов

Рустам Асқарұлы, Айдана Абилова, Арман Сыздықов, Хуралай Молдамурат

Аннотация. Оценка состояния растительного покрова является ключевой задачей точного земледелия, экологии и управления экологическими рисками. Нормализованный разностный вегетационный индекс (NDVI), вычисляемый по отражательной способности в красном и ближнем инфракрасном (NIR) диапазонах, остается базовым физически интерпретируемым показателем для диагностики жизнеспособности растений и выявления стрессовых состояний. Однако применение NDVI в бюджетных сценариях ограничено необходимостью использования мультиспектральных датчиков с NIR-каналом. В работе выполнено сравнение трех подходов: (i) классического NDVI, (ii) преобразования на основе только RGB-каналов и (iii) синтезированного гибридного метода, переносящего принцип нормализации NDVI в модель с доминированием зеленого канала для стандартных RGB-камер. Показаны математические выводы, радиометрическая интерпретация, требования к калибровке и анализ распространения ошибок. Предложен практический UAV-ориентированный рабочий процесс, включающий геометрическую коррекцию, радиометрическую нормализацию, фильтрацию шума и компенсацию освещенности. В качестве примера прикладного использования рассмотрены сценарии оперативной оценки состояния растительности (в т.ч. после чрезвычайных событий), однако не являются основным фокусом исследования. Результаты показывают, что классический NDVI предпочтителен для количественной биофизической интерпретации, тогда как RGB-методы обеспечивают приемлемую качественную сегментацию при ограниченных ресурсах. Синтезированный алгоритм улучшает выделение растительности по сравнению с базовыми RGB-преобразованиями и может применяться при отсутствии NIR-датчиков.

Ключевые слова: NDVI, БПЛА, обработка RGB-изображений, мониторинг растительности, мультиспектральная съемка, радиометрическая калибровка, экологический мониторинг.